Robust Thermal Boundary Condition Using Maxwell-Boltzmann Statistics and its Application

Jae Wan Shim[a] and Renée Gatignol[b]

[a]*Interdisciplinary Fusion Technology Division, Korea Institute of Science and Technology, 136-791, Seoul, Republic of Korea*
[b]*Institut Jean le Rond d'Alembert, Université Pierre et Marie Curie & CNRS, 4 Place Jussieu, 75005 Paris, France*

Abstract. We study a thermal boundary condition which is robust and applicable to a wall along which temperature varies. A framework to derive robust thermal boundary conditions using the Maxwell-Boltzmann statistics is proposed for the purpose of the thermal boundary condition of the discrete kinetic theory. The thermal exchange between fluid particles and walls is achieved by using the relation between the velocity change rate and temperature so that we can control the velocity change rate according to a given temperature boundary condition. We simulated microchannel flows by the lattice gas cellular automata and the direct simulation of Monte Carlo.

Keywords: Thermal boundary condition, discrete kinetic theory, Maxwell-Boltzmann statistics.
PACS: 47.11.-j, 02.50.Cw, 05.20.Dd

INTRODUCTION

The flow in a microchannel is an attractive subject because this has various phenomena still difficult to simulate and the development of microscale devices stimulates the need of this study. The boundary condition is one of the important theme to understand the microchannel flow. The thermal exchange between fluid particles and walls can be described by the velocity change of the fluid particles after their collision to walls. In the paper [1], we derived the relation between the velocity change rate and temperature. By using this relation, we simulated microchannel flows having a thermal boundary condition to a wall along which temperature varies by the lattice gas cellular automata. In this paper, we shortly introduce the derivation of a relation between the velocity change rate of particles and a given temperature. This relation was obtained for the 19-velocities model, which is hexagonal and two-dimensional by using the Maxwell-Boltzmann statistics. We introduce the simulation results obtained by the lattice gas cellular automata [1]. In addition, we present the simulation results obtained by the direct simulation of Monte Carlo (DSMC). The thermal boundary condition used in the simulation of the DSMC is different from that used in the simulation of the lattice gas cellular automata.

RELATION BETWEEN VELOCITY CHANGE RATE AND TEMPERATURE

This is a summary presented in the paper [1] in which the detailed explanation is given. We define discrete velocities of a two-dimensional model in a general form by

$$\vec{v}_i = \begin{cases} c_0(\cos(i\theta_0+\delta_0),\sin(i\theta_0+\delta_0)) \text{ where } i=n_{-1}+1 \text{ to } n_0 \\ c_1(\cos(i\theta_1+\delta_1),\sin(i\theta_1+\delta_1)) \text{ where } i=n_0+1 \text{ to } n_1 \\ c_k(\cos(i\theta_k+\delta_k),\sin(i\theta_k+\delta_k)) \text{ where } i=n_{k-1}+1 \text{ to } n_k \\ \ldots\ldots \\ c_m(\cos(i\theta_m+\delta_m),\sin(i\theta_m+\delta_m)) \text{ where } i=n_{m-1}+1 \text{ to } n_m \end{cases} \quad (1)$$

where $0 \le c_0 < c_1 < c_2 < ..... < c_m$ and $n_{-1} = -1$. If we consider a homogeneous lattice space, it is natural that we have a property of θ_k which is $(n_k - n_{k-1})\theta_k = 2\pi$ where $k = 1, 2, \cdots, m$. We define a rate of velocity change $\mathrm{P}_{\alpha,\beta}$ from $\vec{v}_\alpha$ to $\vec{v}_\beta$ as a result of the heat exchange between a site on a boundary and molecules which collide with the site. The velocity $\vec{v}_\alpha$ corresponds to the incident molecule and $\vec{v}_\beta$ to the reflected molecule.

We make two hypotheses **H₁)** and **H₂)**.

H₁) When the particle colliding with a wall is heated, i.e., the temperature τ_0 before interaction with the wall is lower than the boundary wall temperature τ_w at a position on a wall, we assume that $\mathrm{P}_{\alpha,\beta} = 0$ when $|\vec{v}_\alpha| \ge |\vec{v}_\beta|$ and $\mathrm{P}_{\alpha,\beta} \ge 0$ when $|\vec{v}_\alpha| < |\vec{v}_\beta|$ for the case of $\alpha \ne \beta$. If $\alpha = \beta$, it is possible that $\mathrm{P}_{\alpha,\beta} > 0$ because $\mathrm{P}_{k,k}$ indicates the rate of molecules which maintain their initial velocity. Similarly, when the particle colliding with a wall is cooled, i.e., the flow temperature τ_0 is higher than the boundary wall temperature τ_w, we assume that $\mathrm{P}_{\alpha,\beta} \ge 0$ when $|\vec{v}_\alpha| > |\vec{v}_\beta|$ and $\mathrm{P}_{\alpha,\beta} = 0$ when $|\vec{v}_\alpha| \le |\vec{v}_\beta|$ for the case of $\alpha \ne \beta$. A temperature gradient can be implanted on a wall by adjusting $\mathrm{P}_{\alpha,\beta}$.

We define an index set $\{c_k\}$, utilizing a velocity amplitude c_k in Formula (1), by $\{c_k\} = \{n_{k-1}+1, n_{k-1}+2, \cdots, n_k\}$ where $k = 0, 1, 2, \cdots, m$. In addition, an element of $\{c_k\}$ is defined by $\overline{c}_k \in \{c_k\}$, i.e., a certain index in the index set of $\{c_k\}$. We will use this definition, for example, $\mathrm{P}_{\alpha,\overline{c}_k} \in \left\{\mathrm{P}_{\alpha,i} \mid i \in \{c_k\}\right\}$. We define the number density f_i by the number of molecules, having the discrete velocity $\vec{v}_i$, per unit volume. Generally, we can say

$$f_k(\tau, \vec{u}) = \sum_{i=0}^{n_m} \mathrm{P}_{i,k} f_i(\tau_0, \vec{u}) \text{ where } k = 0, 1, 2, \cdots, n_m. \tag{2}$$

Formula (2) shows that the number density at temperature τ, can be described with the number densities at temperature τ_0. At temperature τ, the molecules having a discrete velocity $\vec{v}_k$ are composed of some of the molecules having a discrete velocity $\vec{v}_k$ at τ_0, i.e. $\mathrm{P}_{k,k} f_k(\tau_0, \vec{u})$ and the molecules initially having discrete velocities $\vec{v}_i$ where $i \ne k$ at τ_0 but becoming $\vec{v}_k$, i.e. $\sum_{i=0,\, i\ne k}^{n_m} \mathrm{P}_{i,k} f_i(\tau_0, \vec{u})$.

H₂) When $\vec{u} \approx 0$;

(1) $\mathrm{P}_{\overline{c}_0,\alpha} = \mathrm{P}_{\overline{c}_0,\beta}$ where $\alpha, \beta \in \{c_k\}$ and $k = 1, 2, \cdots, m$.

(2) $\mathrm{P}_{\overline{c}_l,\overline{c}_p} = \mathrm{P}_{\theta(\overline{c}_l,\overline{c}_p)}$ where $\theta(\overline{c}_l, \overline{c}_p) = \cos^{-1}\left(\dfrac{\vec{v}_{\overline{c}_l} \cdot \vec{v}_{\overline{c}_p}}{|\vec{v}_{\overline{c}_l}||\vec{v}_{\overline{c}_p}|}\right)$.

(3) $f_\alpha(\tau, \vec{u}) = f_\beta(\tau, \vec{u})$ where $\alpha, \beta \in \{c_k\}$ and $k = 0, 1, 2, \cdots, m$.

We define $G_{l,p}$ by the relation $\mathrm{P}(\overline{c}_l, [\overline{c}_p]) = G_{l,p}\mathrm{P}(\overline{c}_l, [\overline{c}_{l+1}])$ where $G_{l,l+1} = 1$. The physical meaning of $G_{l,p}$ is the ratio between the probability sum of the velocity amplitude change from $\overline{c}_l$ to $\overline{c}_p$ and that from $\overline{c}_l$ to $\overline{c}_{l+1}$.

If we apply **H₂** on Formula (2), we obtain

$$f_{\overline{c}_0}(\tau, \vec{u}) = \left(1 - \mathrm{P}([\overline{c}_0], \overline{c}_1)\sum_{p=1}^{m} G_{0,p}\right) f_{\overline{c}_0}(\tau_0, \vec{u}), \tag{3}$$

$$f_{\overline{c}_k}(\tau, \vec{u}) = \left(1 - \mathrm{P}(\overline{c}_k, [\overline{c}_{k+1}])\sum_{p=1}^{m-k} G_{k,k+p}\right) f_{\overline{c}_k}(\tau_0, \vec{u}) + \sum_{l=0}^{k-1} \mathrm{P}([\overline{c}_l], \overline{c}_k) f_{\overline{c}_l}(\tau_0, \vec{u}) \tag{4}$$

where $k = 1,2,...,m-1$ and

$$f_{\bar{c}_m}(\tau,\vec{u}) = f_{\bar{c}_m}(\tau_0,\vec{u}) + \sum_{l=0}^{m-1} \mathrm{P}([\bar{c}_l],\bar{c}_m) f_{\bar{c}_l}(\tau_0,\vec{u}) \,. \tag{5}$$

We define $\mathrm{P}(\bar{c}_l,[\bar{c}_p]) = \sum_{i=n_{p-1}+1}^{n_p} \mathrm{P}_{\bar{c}_l,i}$ and $\mathrm{P}([\bar{c}_l],\bar{c}_p) = \sum_{i=n_{l-1}+1}^{n_l} \mathrm{P}_{i,\bar{c}_p}$. Let's consider a specific case of 19-velocities model where the discrete velocities are given by

$$\vec{v}_i = \begin{cases} (0,0) & \text{where i = 0} \\ c'(\cos(\pi i/3),\sin(\pi i/3)) & \text{where i = 1,2,3,4,5,6} \\ \sqrt{3}c'(\cos(\pi i/3+\pi/6),\sin(\pi i/3+\pi/6)) & \text{where i = 7,8,9,10,11,12} \\ 2c'(\cos(\pi i/3),\sin(\pi i/3)) & \text{where i = 13,14,15,16,17,18} \end{cases} . \tag{6}$$

If we express $\mathrm{P}(\bar{c}_l,[\bar{c}_p])$ by the density distributions from Formulas (3), (4), and (5); and basic calculations [1], we have,

$$\mathrm{P}(\bar{c}_0,[\bar{c}_1]) = \frac{f_{\bar{c}_0}(\tau_0,\vec{u}) - f_{\bar{c}_0}(\tau,\vec{u})}{f_{\bar{c}_0}(\tau_0,\vec{u})(1+G_{0,2}+G_{0,3})} \tag{7}$$

and

$$\mathrm{P}(\bar{c}_1,[\bar{c}_2]) = \frac{1}{f_{\bar{c}_1}(\tau_0,\vec{u})(1+G_{0,2}+G_{0,3})(1+G_{1,3})} \times \left\{ \left\{ f_{\bar{c}_1}(\tau_0,\vec{u}) - f_{\bar{c}_1}(\tau,\vec{u}) \right\} (1+G_{0,2}+G_{0,3}) + f_{\bar{c}_0}(\tau_0,\vec{u}) - f_{\bar{c}_0}(\tau,\vec{u}) \right\} . \tag{8}$$

Finally

$$\begin{aligned} \mathrm{P}(\bar{c}_2,[\bar{c}_3]) = \frac{1}{f_{\bar{c}_2}(\tau_0,\vec{u})(1+G_{0,2}+G_{0,3})(1+G_{1,3})} \times \\ \left\{ \left(f_{\bar{c}_0}(\tau_0,\vec{u}) - f_{\bar{c}_0}(\tau,\vec{u}) \right)(1+G_{0,2}+G_{0,2}G_{1,3}) \right. \\ + \left(f_{\bar{c}_1}(\tau_0,\vec{u}) - f_{\bar{c}_1}(\tau,\vec{u}) \right)(1+G_{0,2}+G_{0,3}) \\ \left. + \left(f_{\bar{c}_2}(\tau_0,\vec{u}) - f_{\bar{c}_2}(\tau,\vec{u}) \right)(1+G_{0,2}+G_{0,3})(1+G_{1,3}) \right\}. \end{aligned} \tag{9}$$

According to the solution of the two-dimensional hexagonal 19-velocities model of the thermal lattice Boltzmann method [2], we can obtain $f_{\bar{c}_k}(\tau,\vec{u})$ and $f_{\bar{c}_k}(\tau_0,\vec{u})$ in Formulas (7), (8), and (9). When $\vec{u} \approx 0$, we can substitute them by

$$f_{\bar{c}_0}(\tau_0,\vec{0}) = \frac{n}{3} w_0 \,,\ f_{\bar{c}_0}(\tau,\vec{0}) = \frac{nw_0}{3}\left\{1-(\tilde{\tau}-1)+(\tilde{\tau}-1)^2\right\},\ f_{\bar{c}_1}(\tau_0,\vec{0}) = \frac{nw_1}{3},$$

$$f_{\bar{c}_1}(\tau,\vec{0}) = \frac{nw_1}{3}\left\{1+(\tilde{\tau}-1)(-1+r^2)+\frac{(\tilde{\tau}-1)^2}{2}(2-4r^2+r^4)\right\},\ f_{\bar{c}_2}(\tau_0,\vec{0}) = \frac{nw_2}{3},$$

$$f_{\bar{c}_2}(\tau,\vec{0}) = \frac{nw_2}{3}\left\{1+(\tilde{\tau}-1)(-1+3r^2)+\frac{(\tilde{\tau}-1)^2}{2}(2-12r^2+9r^4)\right\},\ f_{\bar{c}_3}(\tau_0,\vec{0}) = \frac{nw_3}{3} \text{ and}$$

$$f_{\bar{c}_3}(\tau,\vec{0}) = \frac{nw_3}{3}\left\{1+(\tilde{\tau}-1)(-1+4r^2)+\frac{(\tilde{\tau}-1)^2}{2}(2-16r^2+16r^4)\right\}$$

where $\tilde{\tau} = \tau / \tau_0$, $w_0 = 0.164$, $w_1 = 0.310$, $w_2 = 0.011$, $w_3 = 0.015$ and $r = 1.115$.

We should find $G_{l,p}$ in Formulas (7), (8), and (9). For this purpose, we define $N_{\alpha\beta}$ by the number of particles which change their velocity amplitude from c_α to c_β after collision with a wall and by analogy $N_{\alpha\delta}$ from c_α to c_δ in general cases of a discrete velocity system. When the heat transferred from the wall to the particles is ΔE, the number of possible cases for the combination of $N_{\alpha\beta}$ and $N_{\alpha\delta}$ is $W = \frac{(N_{\alpha\beta} + N_{\alpha\delta})!}{N_{\alpha\beta}!\, N_{\alpha\delta}!}$ and the transferred heat is $\Delta E = N_{\alpha\beta}\varepsilon_{\alpha\beta} + N_{\alpha\delta}\varepsilon_{\alpha\delta}$ where $\varepsilon_k = \frac{m}{2} {c_k}^2$, $\varepsilon_{\alpha\beta} = \varepsilon_\beta - \varepsilon_\alpha = \frac{m\left({c_\beta}^2 - {c_\alpha}^2\right)}{2}$ and $\varepsilon_{\alpha\delta} = \varepsilon_\delta - \varepsilon_\alpha = \frac{m\left({c_\delta}^2 - {c_\alpha}^2\right)}{2}$. We can calculate the most probable case by virtue of the Lagrange multiplier denoted by χ. We define

$$\mathrm{L} = \ln W + \chi(\Delta E - N_{\alpha\beta}\varepsilon_{\alpha\beta} - N_{\alpha\delta}\varepsilon_{\alpha\delta}) \tag{10}$$

then the constraint $\frac{\partial \mathrm{L}}{\partial N_{\alpha\beta}} = \frac{\partial \mathrm{L}}{\partial N_{\alpha\delta}} = 0$ must be satisfied. We use the Sterling approximation $N! = N^N e^{-N}$. We then obtain

$$\frac{\partial \mathrm{L}}{\partial N_{\alpha\beta}} = \ln(N_{\alpha\beta} + N_{\alpha\delta}) - \ln N_{\alpha\beta} - \chi\varepsilon_{\alpha\beta} = 0 \tag{11}$$

and

$$\frac{\partial \mathrm{L}}{\partial N_{\alpha\delta}} = \ln(N_{\alpha\beta} + N_{\alpha\delta}) - \ln N_{\alpha\delta} - \chi\varepsilon_{\alpha\delta} = 0\,. \tag{12}$$

Note that $G_{0,2} = \frac{\mathrm{P}([\bar{c}_0], \bar{c}_2)}{\mathrm{P}([\bar{c}_0], \bar{c}_1)} = \frac{N_{02}}{N_{01}}$ and $\varepsilon_2 = 3\varepsilon_1$ for the 19-velocities model defined by Formula (6). Therefore, when $\alpha = 0$, $\beta = 1$ and $\delta = 2$, Formulas (11) and (12) become $\ln(1 + G_{0,2}) = \chi\varepsilon_1$ and $\ln(\frac{1}{G_{0,2}} + 1) = 3\chi\varepsilon_1$, respectively. If we eliminate $\chi\varepsilon_1$ in the last two equations, we obtain

$$\frac{1}{G_{0,2}} + 1 = (1 + G_{0,2})^3\,. \tag{13}$$

Formula (13) has a positive real valued root $G_{0,2} \approx 0.466$, which is the only positive root. Similarly, we can obtain the values of $G_{l,p}$. We derived the velocity change rate as Formula (14) for 19-velocities model. This is for the case of heating by collision.

$$\begin{aligned}
&\mathrm{P}(\bar{c}_0, [\bar{c}_1]) = -0.54(2 - 3\tilde{\tau} + \tilde{\tau}^2),\ \mathrm{P}(\bar{c}_0, [\bar{c}_2]) = -0.25(2 - 3\tilde{\tau} + \tilde{\tau}^2) \\
&\mathrm{P}(\bar{c}_0, [\bar{c}_3]) = -0.21(2 - 3\tilde{\tau} + \tilde{\tau}^2),\ \mathrm{P}(\bar{c}_1, [\bar{c}_2]) = 0.24(-1 + \tilde{\tau})(-0.90 + \tilde{\tau}) \\
&\mathrm{P}(\bar{c}_1, [\bar{c}_3]) = 0.18(-1 + \tilde{\tau})(-0.90 + \tilde{\tau}),\ \mathrm{P}(\bar{c}_2, [\bar{c}_3]) = 2.60(-1 + \tilde{\tau})(-0.33 + \tilde{\tau})
\end{aligned} \tag{14}$$

SIMULATION RESULTS

We performed a simulation by the lattice gas cellular automata using Formula (14). Figure 1 shows the thermal boundary condition implanted on the longitudinal wall of the microchannel. The left half of the longitudinal wall of the microchannel has a decreasing temperature gradient. The right half is an adiabatic wall. Figure 2 shows the temperature distribution. This figure shows only the half of the microchannel with respect to the longitudinal central axis. The dimension of the microchannel is $1\mu m$ width and $10\mu m$ length, connected with two chambers of $2\mu m$ length. The bounce-back reflection scheme is used on the wall. The entrance boundary values of pressure, density, temperature, and velocity are identical to the exit ones. Therefore, there is no significant pressure or velocity

gradient on the calculation domain. We observe that the left part of the microchannel is heated according to the implanted boundary condition.

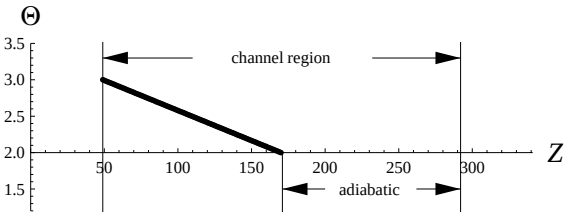

FIGURE 1. The thermal boundary condition implanted on the longitudinal wall [1].

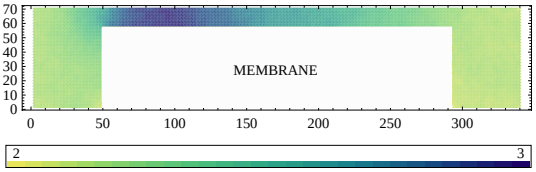

FIGURE 2. The temperature distribution in the microchannel [1].

Figures 3 and 4 show the thermal boundary condition and the corresponding temperature distribution, respectively. Note that the other conditions are same to the previous case of Figures 1 and 2. We observe that the central part of the microchannel is heated according to the implanted boundary condition.

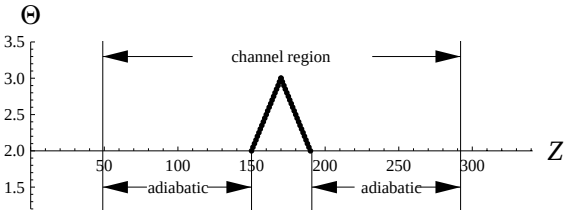

FIGURE 3. The thermal boundary condition implanted on the longitudinal wall [1].

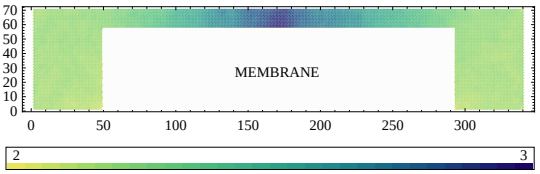

FIGURE 4. The temperature distribution in the microchannel [1].

Figures 5, 6, and 7 show the pressure, temperature, and longitudinal velocity distributions obtained by the DSMC, respectively. The dimension of the microchannel is $1\mu m$ width and $10\mu m$ length, connected with two chambers of $7\mu m$ length. The diffuse reflection scheme is used. Along the wall of the microchannel, the given thermal boundary condition is that temperature decreases linearly from 500K to 300K. The entrance initial boundary values are 500K, 1.3×10^5 Pa, and the number density of 1.88×10^{25}. The exit initial boundary values are 300K, 1.0×10^5 Pa, and the number density of 2.41×10^{25}. The horizontal axis Z represents the normalized longitudinal position and the vertical axis represents the normalized pressure and temperature in Figures 5 and 6; and longitudinal velocity in Figure 7.

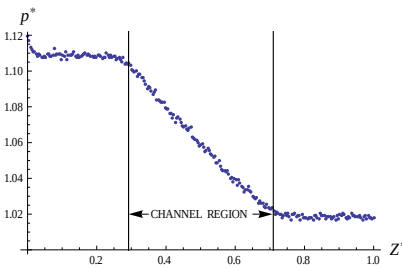

FIGURE 5. Pressure distribution.

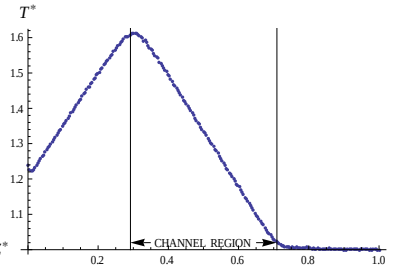

FIGURE 6. Temperature distribution.

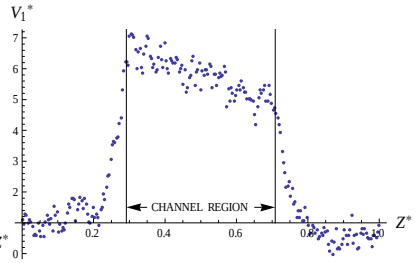

FIGURE 7. Longitudinal velocity distribution.

Figures 8, 9, and 10 show the pressure, temperature, and longitudinal velocity distributions obtained by the DSMC, respectively, as Figures 5, 6, and 7. However, several conditions are different. The length of the two chambers is $2\mu m$ in common. The walls are adiabatic. The entrance initial boundary values are 330K, $1.1\times1.3\times10^5$ Pa, and the number density of 3.14×10^{25}. The exit initial boundary values are 300K, 1.3×10^5 Pa, and

the number density of 3.14×10^{25}. We can observe that the temperature in the channel region is constant in contrast to the temperature profile having a steep slope in Figure 6.

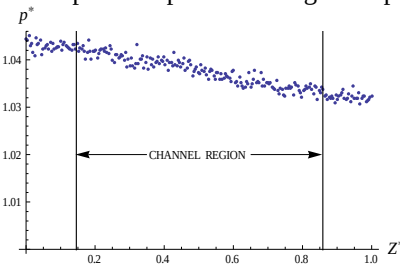

FIGURE 8. Pressure distribution.

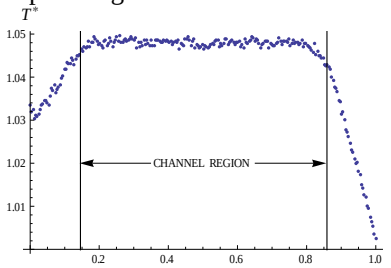

FIGURE 9. Temperature distribution.

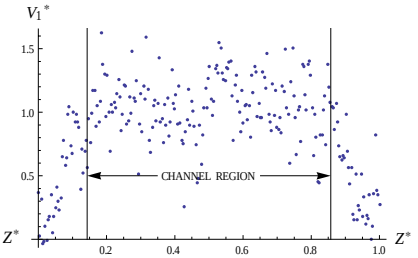

FIGURE 10. Longitudinal vel. distribution.

CONCLUSION

We studied a thermal boundary condition which is robust and applicable to a wall along which temperature varies. A framework to derive robust thermal boundary conditions using the Maxwell-Boltzmann statistics was proposed for the purpose of the thermal boundary condition of the discrete kinetic theory. The thermal exchange between fluid particles and walls was achieved by using the relation between the velocity change rate and temperature so that we could control the velocity change rate according to a given temperature boundary condition. We had simulated microchannel flows by the lattice gas cellular automata and lattice Boltzmann method [3, 4]. However, the results in the paper [3] did not treat the thermal boundary condition on walls and the results in the paper [4] did not relate the temperature and the velocity change rate. In this paper, we related the temperature and the velocity change rate. In addition, we obtained the simulation results by the direct simulation of Monte Carlo.

ACKNOWLEDGMENT

This research was partially supported by the KIST Institutional Program.

REFERENCES

1. J. W. Shim and R. Gatignol, *Phys. Rev. E* 81, 046703 (2010)
2. J. W. Shim, “Modelisation of Flows through Microchannels by Cellular Automata and Lattice Boltzmann Method”, Ph.D. Thesis, Université Pierre et Marie Curie, Paris VI, 2008.
3. J. W. Shim and R. Gatignol, *Houille Blance* **5**, 120 (2009).
4. J. W. Shim and R. Gatignol, “Microchannel Flow With Lattice Gas Cellular Automata and Lattice Boltzmann Method” in the 26th *International Symposium on Rarefied Gas Dynamics*, edited by T. Abe, AIP Conference Proceedings 1084, American Institute of Physics, Melville, NY, 2009, pp. 1033.